Chemical Functionalization of Cadmium Sulfide Quantum-Confined Microclusters

Horst Noglik and William J. Pietro*

Department of Chemistry, York University
4700 Keele St., North York (Toronto)
Ontario, Canada, M3J 1P3

Received April 20, 1994
Revised Manuscript Received June 6, 1994

Semiconductor clusters of nanometer dimensionality have been known for almost a century[1] and remain among the most intriguing classes of electronic materials. Much recent attention has focused on quantum size effects and systematic investigations have revealed important size and dimensionality dependent properties.[2] In particular, when the particle size is reduced below the Bohr radius of the lowest lying exciton state, dramatic changes to the material's optical properties are effected. Such particles have been termed "quantum dots". The quantum confinement of conduction electrons impart many novel properties to these systems such as single-electron-transistor properties, enhanced nonlinear optical activities, and increased bandgaps.[3-6] These properties can be modified by "bandgap tailoring", which is enacted predictably by altering the diameter of the cluster.

Quantum dots have been generated by numerous methods including molecular beam epitaxy, MOCVD, microlithography, and direct chemical preparation. However, one of the most widely employed methods involves formation in a matrix, such as a zeolite or inverted micelle,[7] or by use of a kinetic trapping agent such as thiophenol.[8] Much progress has been made in the optimization of kinetic trapping conditions, and it is currently possible to obtain well-characterized CdS microclusters with very narrow size distributions. Further refinement of particle size can be accomplished through size exclusion chromatography or gel electrophoresis.[8]

While the naturally capped clusters formed by kinetic trapping techniques show much promise, a major drawback is the lack of suitable methods to implement the quantum dots into specific arrays, or selectively attach additional moieties such as "wires" to the clusters. We report here the first surface functionalization of a CdS quantum dot through which a variety of moieties may be tethered.

In the kinetic trapping method, CdS is precipitated from a solution of cadmium acetate and sodium sulfide in the presence of thiophenol, resulting in CdS microclusters (with a relatively high degree of monodispercity) trapped in shells of thiophenol. We have found that substitution of *n*% of the thiophenol molecules in solution by 4-mercaptopyridine results in formation of pyridine-functionalized microclusters of the general formula $[CdS_x(S\phi,n\%Spy)_y]$, incorporating approximately *n*% pyridine functionality on the surface of the encapsulated CdS quantum dot. Hence, reaction of 50 mL of 50 mM $Na_2S{\cdot}9H_2O$ with 0.1 M $Cd(OAc)_2{\cdot}2H_2O$ in the presence of 46 mL of 0.2 M thiophenol and 4 mL of 0.2 M 4-mercaptopyridine (8% of total moles of capping agent) in 2:1:1 $H_2O/CH_3OH/CH_3CN$ under deoxygenated argon yielded thiophenol-capped CdS microclusters with approximately 8% pyridine surface functionality (calculated for $CdS_{0.4}(SC_6H_5)_{0.86}(SC_5H_4N)_{0.11}$: Cd, 48.61; S, 19.00; C, 29.66; H, 2.07; N, 0.67; found: Cd, 48.6; S, 17.93; C, 29.85; H, 2.17; N, 0.83; $[CdS_x(S\phi,n\%Spy)_y]$, $n = 11$). Integration of the aromatic proton signals in the ^1H NMR in DMSO-d_6 (Figure 1) indicates a surface functionality of approximately 7.8%. The chemical shifts are typical for the α-hydrogens of a pyridine residue, and the absence of a signal downfield of 9 ppm indicates no appreciable amount of N-bound mercaptopyridine. Further evidence for sulfur as the primary site of microcluster coordination was obtained from a control experiment in which the mercaptopyridine was replaced by pyridine in the kinetic trapping reaction mixture. After workup, which involved repeated washing and centrifugation, the ^1H NMR spectrum showed no detectable pyridine signals. It is nevertheless likely that pyridine does possess some ability to chemisorb to the microcluster through nitrogen, as the solubility properties of the functionalized and unfunctionalized microclusters are somewhat different. In DMSO both form clear nonturbid microsuspensions which exhibit a pronounced Tyndall effect, whereas in CH_3CN, the functionalized microcluster suspensions possess markedly greater turbidity and show much greater sedimentations rates than the unfunctionalized systems. These observations suggest that the pyridine-capped microclusters have a greater propensity for aggregation and, possibly, cross-linking.

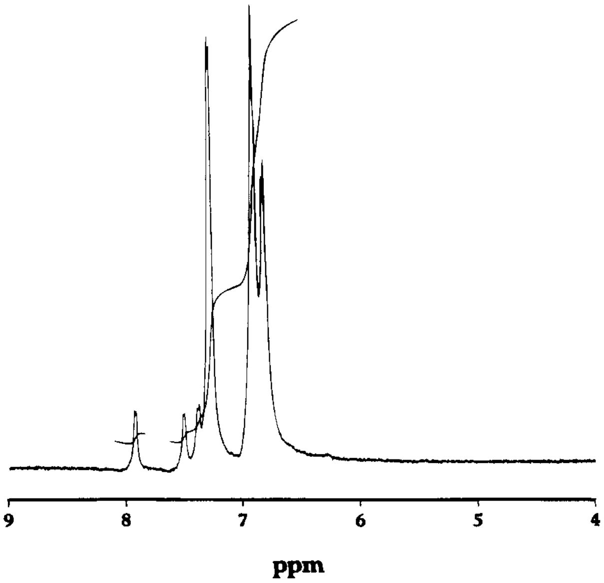

Figure 1. ^1H NMR spectrum for $[CdS_x(S\phi,8\%Spy)_y]$ in DMSO-d_6.

The location of the absorption edge (350 nm) in the electronic spectrum (Figure 2) indicates a cluster diam-

---

(1) Ostwald, W. *Die Welt der vernaschlässigten Dimensionen*; Steinkopf: Dresden, 1915.

(2) Weller, H. *Angew. Chem., Int. Ed. Engl.* **1993**, *32*, 41.

(3) Gleiter, H. *Phys. Bl.* **1991**, *47*, 753.

(4) Henglein, A. *Top. Curr. Chem.* **1988**, *143*, 113.

(5) Henglein, A. *Chem. Rev.* **1989**, *89*, 1861.

(6) Brus, L. E. *Appl. Phys. A* **1991**, *53*, 465.

(7) (a) Steigerwald, M. L.; Brus, L. E. *Acc. Chem. Res.* **1990**, *23*, 183. (b) Ozin, G. A. *Adv. Mater.* **1992**, *4*, 612. (c) Fendler, J. H. *Chem. Rev.* **1987**, *87*, 877.

(8) Herron, N.; Wang, Y.; Eckert, H. *J. Am. Chem. Soc.* **1990**, *112*, 1322.

0897-4756/94/2806-1593$04.50/0

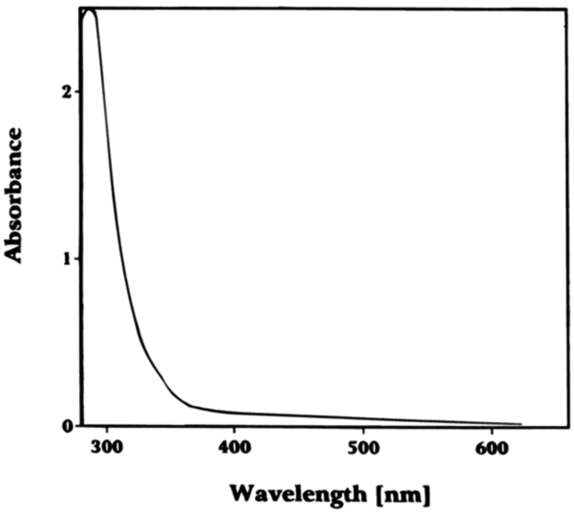

Figure 2. Electronic absorption spectrum for [$CdS_x(S\phi,8\%Spy)_y$] in CH_3CN.

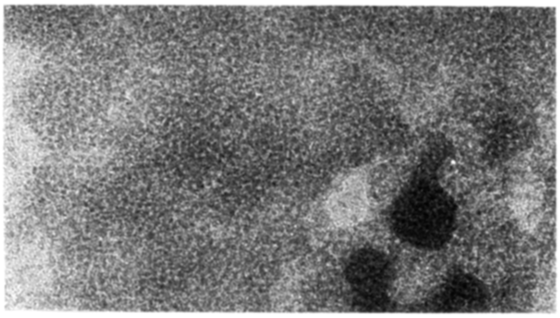

Figure 3. TEM image of [$CdS_x(S\phi,8\%Spy)_y$] microclusters. Scale: 5 mm = 1000 Å.

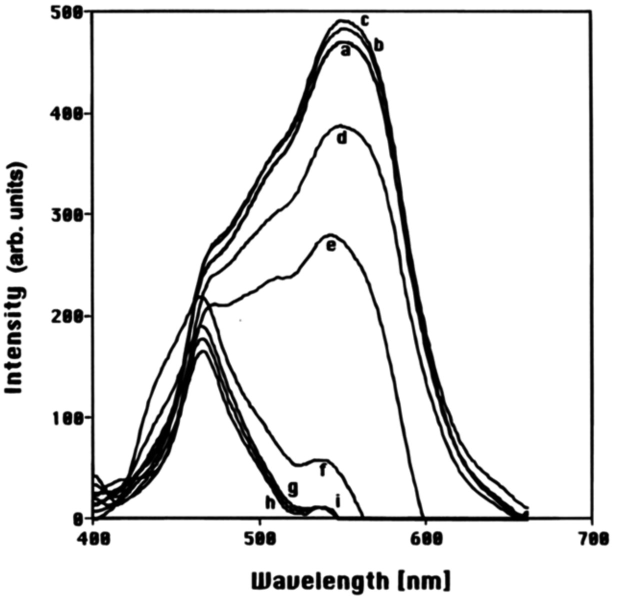

Figure 4. Fluorescence spectra of 1.0 mg/mL [$CdS_x(S\phi,n\%Spy)_y$] in CH_3CN, at $n = 0$ (a), 1 (b), 2 (c), 3 (d), 4 (e), 5 (f), 6 (g), 7 (h), and 8 (i).

Table 1. AM1/CISD Calculated Highest Occupied Molecular Orbital and Acceptor State Energies (in Electronvolts) for Moieties 1–3

molecule	E_{homo}	S_1	$E_{acceptor}$
1	−2.92	2.79	−0.13
2	−3.33	2.76	−0.57
3	−7.98	3.00	−4.98

eter of 17 Å, consistent with unfunctionalized thiophenol-encapsulated CdS microclusters prepared under similar conditions (typically 10–30 Å).[8] This size estimation was confirmed by transmission electron micrographs (Figure 3) indicating cluster sizes of 20 ± 4 Å diameter.

The effects of pyridine functionality on the luminescence spectrum of the CdS microcluster is most interesting. Figure 4 shows the fluorescence spectra (excitation $\lambda = 350$ nm) of 17 Å [$CdS_x(S\phi,n\%Spy)_y$] microclusters for $n = 0$–8%. With $n = 0$, two characteristic emissions are observed at 557 and 470 nm, which have been assigned as trap-induced electron–hole recombination and recombination from an excitonic state, respectively.[9] The presence of increasing surface pyridine increasingly quenches the trap-induced fluorescence, while leaving the excitonic fluorescence unaffected. This observation is consistent with the previously reported assertion that trap states are localized at the surface of encapsulated semiconductor microclusters and are relatively long lived.[9a] Addition of pyridine to a CH_3CN suspension of unfunctionalized thiophenol-capped CdS microcluster resulted in no observed quenching of the 557 nm band. Ab initio HF/3-21G*//3-21G* calculations on thiophenoxide, **1**, pyridine-4-sulfide, **2**, and pyridinium-4-sulfide, **3**, suggest that the mechanism for the quenching of the 557 nm fluorescence proceeds via destruction of the surface-trapped state by electron capture. The calculations also suggest that the accepting species is likely to be small amounts of protonated or metalated pyridine rather than pyridine. The LUMO of **2** is calculated to lie only 0.25 eV below that of **1**, whereas the LUMO is lowered by an additional 5.9 eV upon protonation of **2**. The calculations suggest that it is unlikely that hole capture is involved in the quenching mechanism, as the HOMO energy is successively lowered in going from **1** (−1.63 eV) to **2** (−2.37 eV) to **3** (−7.57 eV). In addition to the 3-21G* results, the acceptor state energies of moieties **1–3** were directly calculated by the method of limited configuration interaction over singles and doubles (CISD) at the semiempirical AM1 level. Table 1 presents the results of the AM1/CISD calculations. These data clearly show that the energy of the acceptor state of **2** is only slightly lower than that of **1** and is only 0.57 eV below the vacuum level, well above the CdS conduction band edge. However, the energy of the acceptor state of **3** is 4.98 eV below the vacuum level, residing below the Fermi level of CdS (≈4 eV), suggesting again that protonated or metalated pyridine is likely to be involved in the quenching mechanism. Moreover, selective quenching of the 557 nm emission has also been observed by exposure of CdS microclusters to very low concentrations of methylviologen.[9a,10,11]

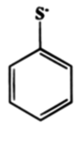

1

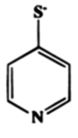

2

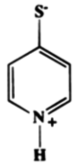

3

---

[9] (a) Fojtik, A.; Weller, H.; Koch, U.; Henglein, A. *Ber. Bunsen-Ges. Phys. Chem.* **1984**, *88*, 969. (b) Chen, W.; McLendon, G.; Marchetti, A.; Rehm, J. M.; Freedhoff, M. I.; Myers, C. *J. Am. Chem. Soc.* **1994**, *116*, 1585.

The activity of the pyridine functionalized CdS microclusters toward coordination to transition-metal species was demonstrated by ligation to chromium phthalocyanine, Cr(Pc), **4**. Metallophthalocyanines have a very strong electronic absorption at ca. 670 nm (Q-band), a region of the spectrum where CdS is virtually transparent. $[CdS_x(S\phi,8\%Spy)_y)]$ (100 mg) was sonicated in a saturated solution of Cr(Pc) in dry, deoxygenated CH_3CN, and left at room temperature for 48 h under argon. The resulting blue-green solid was collected by centrifugation and repeatedly resuspended, sonicated, and centrifuged in CH_3CN until the washings were free of Cr(Pc). The electronic spectrum of a sonicated DMSO microsuspension of the blue-green solid is presented in Figure 5. The spectrum is identical with that of unreacted $[CdS_x(S\phi,8\%Spy)_y]$ except for the appearance of the characteristic Q-band of Cr(Pc) at 676 nm.[12] Unfunctionalized $[CdS_x(S\phi)_y]$ treated in the same manner did not incorporate any detectable Cr(Pc). Fe(Pc) and Zn(Pc) can also be bound in a similar fashion. We have also demonstrated the activity of the surface pyridine functionality by covalent binding to coumarin, **5**, prepared as shown in Scheme 1. Upon excitation of the $[CdS_x(S\phi,8\%Spy)_y]$−coumarin microcluster at 300 nm, the characteristic fluorescence of coumarin at 445 nm is observed. Further studies concerning the use of functionalized semiconductor microclusters as ligands are presently underway in our laboratories and will be the subject of a future publication.

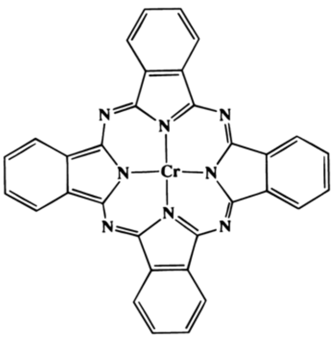

4

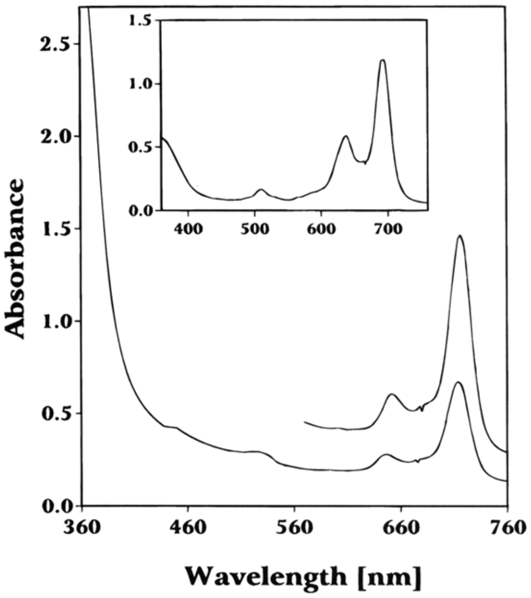

Figure 5. Electronic absorption spectrum for $\{CdS_x(S\phi,8\%Spy)_y[Cr(Pc)]_z\}$ in CH_3CN. Inset: electronic absorption spectrum for pure Cr(Pc) in pyridine.

Scheme 1

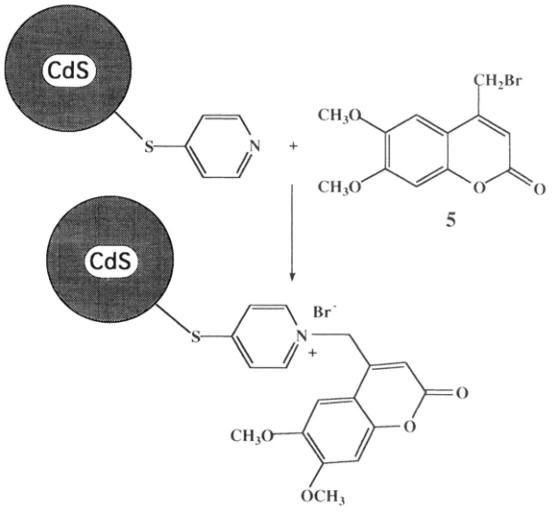

Acknowledgment. We are indebted to Professor A. B. P. Lever, Professor D. V. Stynes, Professor A. Vlcek, and Dr. S. S. Fielder for their helpful discussions and advice. We wish to thank the Natural Science and Engineering Research Council of Canada (NSERC) for their financial support.

---

(10) Weller, H.; Koch, U.; Gutiérrez, M.; Henglein, A. *Ber. Bunsen-Ges. Phys. Chem.* **1984**, *88*, 649.

(11) Grätzel, M. In *Electrochemistry in Colloids and Dispersions*; Mackay, R. A., Texter, J., Eds.; VCH: New York, 1992.

(12) Stillman, M. J.; Nyokong, T. In *Phthalocyanines, Properties and Applications*; Leznoff, C. C., Lever, A. B. P., Eds.; VCH: New York, 1989.